

RESEARCH ARTICLE

# Push Force Analysis of Anchor Block of the Oil and Gas Pipeline in a Single-Slope Tunnel Based on the Energy Balance Method

Yifei Yan<sup>1</sup>, Lisong Zhang<sup>2\*</sup>, Xiangzhen Yan<sup>2</sup>

**1** College of Mechanical and Electronic Engineering, China University of Petroleum, Qingdao 266580, China, **2** College of Pipeline and Civil Engineering, China University of Petroleum, Qingdao 266580, China

\* [lisongzhang1982@163.com](mailto:lisongzhang1982@163.com)

## Abstract

In this paper, a single-slope tunnel pipeline was analysed considering the effects of vertical earth pressure, horizontal soil pressure, inner pressure, thermal expansion force and pipeline—soil friction. The concept of stagnation point for the pipeline was proposed. Considering the deformation compatibility condition of the pipeline elbow, the push force of anchor blocks of a single-slope tunnel pipeline was derived based on an energy method. Then, the theoretical formula for this force is thus generated. Using the analytical equation, the push force of the anchor block of an X80 large-diameter pipeline from the West—East Gas Transmission Project was determined. Meanwhile, to verify the results of the analytical method, and the finite element method, four categories of finite element codes were introduced to calculate the push force, including CAESARII, ANSYS, AutoPIPE and ALGOR. The results show that the analytical results agree well with the numerical results, and the maximum relative error is only 4.1%. Therefore, the results obtained with the analytical method can satisfy engineering requirements.



## OPEN ACCESS

**Citation:** Yan Y, Zhang L, Yan X (2016) Push Force Analysis of Anchor Block of the Oil and Gas Pipeline in a Single-Slope Tunnel Based on the Energy Balance Method. PLoS ONE 11(3): e0150964. doi:10.1371/journal.pone.0150964

**Editor:** Ye Wu, Beijing University of Posts and Telecommunications, CHINA

**Received:** July 31, 2015

**Accepted:** February 21, 2016

**Published:** March 10, 2016

**Copyright:** © 2016 Yan et al. This is an open access article distributed under the terms of the [Creative Commons Attribution License](https://creativecommons.org/licenses/by/4.0/), which permits unrestricted use, distribution, and reproduction in any medium, provided the original author and source are credited.

**Data Availability Statement:** All relevant data are within the paper.

**Funding:** The authors have no support or funding to report.

**Competing Interests:** The authors have declared that no competing interests exist.

## 1. Introduction

In China, West-East gas pipeline system project was constructed to relieve the energy market of eastern cities, having one trunk line with an outside diameter of 1219 mm. To save the engineering costs, the project crosses the complex geological areas, from Tianshan to Nanling. Given that long-distance oil and gas pipelines often pass through complex regions, different methods of crossing mountains were used in engineering. In order to reduce pipeline construction costs, mountain tunnel is commonly constructed to lay the pipeline as a reasonable and effective way. The cost of constructing gas pipelines in tunnels is usually high because the terrain on which the tunnels lie is excessively complex. Tunnel construction effectively reduces gas pipeline construction costs and links different gas tanks. To prevent damage to the tunnel or the pipeline elbow, an anchor block is set in the straight pipeline near the pipeline elbow to limit the thermal expansion displacement of the pipeline [1–3]. This displacement is caused by temperature and pressure. The key factor in anchor block design is to calculate the push force

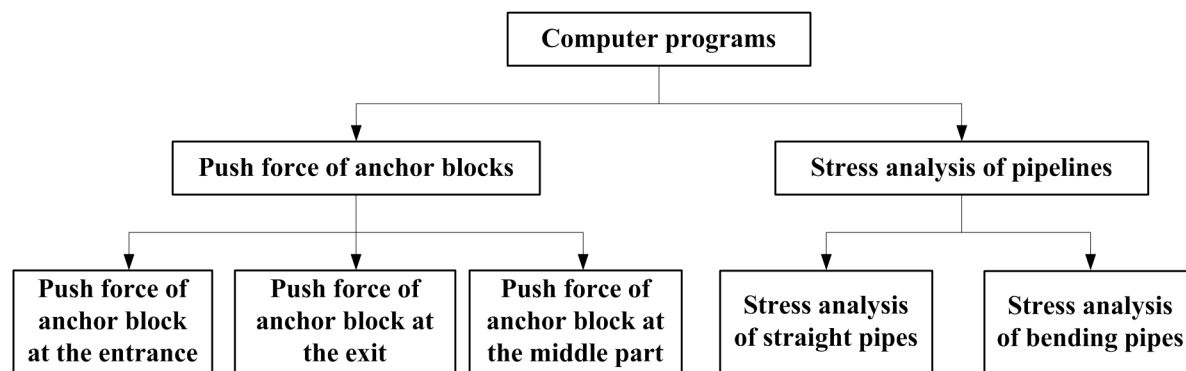


**Fig 1. The schematic diagram of the computer program.**

doi:10.1371/journal.pone.0150964.g001

endured by this block. By searching the work published, it can be found that some researchers performed the design of the anchor block when giving a known push force [4–7]. The push force result can be solved accurately using the finite element software, but achieving this result is difficult for field staff members because of modelling and operation complexities. In this study, the virtual work principle is introduced to derive the analytic model for the anchor push force of a single-slope tunnel pipeline, induced by thermal expansion displacement. In this analysis, the statically indeterminate mechanics model of the bend was established, and the condition of deformation compatibility and the hypothesis of stagnation point were used. The corresponding computer program was developed as well (see Fig 1). The analytical calculation results are compared with the results obtained with finite element software to verify the accuracy of the formula.

## 2. Engineering model of the slope tunnel pipeline

The tunnel pipelines constructed for the West—East Gas Transmission Pipeline Project are laid in various forms. Amongst the slope tunnel pipelines, a vertical elbow is commonly set at the entrance and at the exit of the tunnel. The structural representation and engineering model of these pipelines are shown in Figs 2 and 3, respectively.

A tunnel pipeline with a vertical elbow is located at the tunnel opening. Two elbows are inserted into the ground in the tunnel opening, and the angles are denoted by  $\beta$  and  $\phi$ . The anchor blocks are located at distances of  $L_1$  and  $L_3$  from the external elbow. The sliding anchor

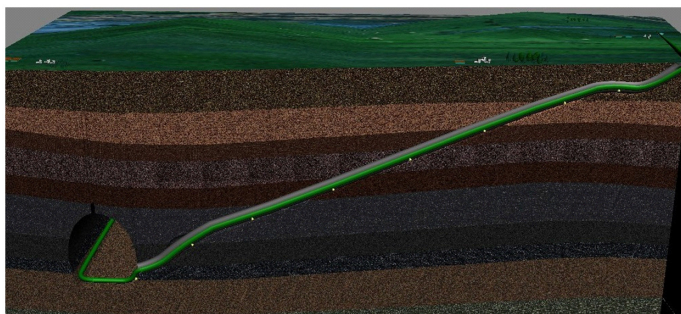


**Fig 2. Structural representation of the single-slope tunnel pipeline in oil and gas engineering.**

doi:10.1371/journal.pone.0150964.g002

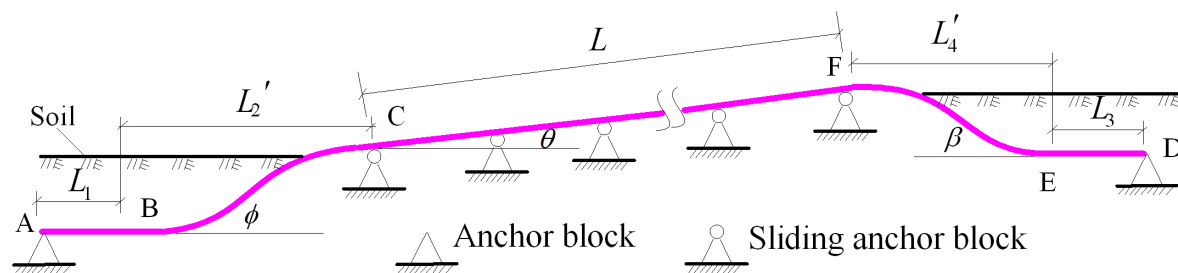


**Fig 3. Engineering model of the slope tunnel pipeline.**

doi:10.1371/journal.pone.0150964.g003

blocks are set continuously inside the tunnel, and the span between them is equal to  $l$ . The total number of span is indicated by  $n$ .

### 3. Mechanical simplification of the engineering model

An anchor block can prevent the pipeline from rotating and moving in any direction. The mechanical model can be modelled as the fixed-end constraint. This kind of constraint can subject the moment, axial force and shear. Meanwhile, the constraint prevents any movement.

A sliding anchor block can provide a supply at the vertical direction for the pipeline. However, this kind of the block does not provide the reaction force along the axial direction of the pipeline; nor does it supply the moment and axial force. Consequently, the pipeline can move along the axial direction. The friction force between the tunnel pipeline and the anchor can, to some extent, prevent the movement tendency of the tunnel pipeline. According to the analysis above, the mechanical model for a sliding anchor block can be simplified as an interface constraint. The accompanying friction force is exerted in the horizontal direction.

If the straight pipe is much longer than the arc-length of an elbow in the tunnel pipeline system, the internal force of the elbow section changes a little. The elbow can reduce to a hinge model, retaining the bending flexibility. This model is called the elastic bending hinge [8], regardless of the elbow size. Assuming that the moment of the elastic bending hinge is denoted by  $M$ , and the change in the bending resistance hinge induced by  $M$  is represented by  $\Delta\phi$ , then  $M$  and  $\Delta\phi$  should have a linear relationship. The corresponding equations are given by [9]

$$M = K \cdot \Delta\phi. \quad (1)$$

$$K = \frac{E\pi r t^2}{1.65\phi}. \quad (2)$$

The effect of the internal pressure can be considered as follows:

$$K = \frac{E\pi r t^2}{1.65\phi} \left[ 1 + \frac{6pr}{Et} \left( \frac{r}{t} \right)^{4/3} \left( \frac{R}{r} \right)^{1/3} \right]. \quad (3)$$

The model of the elastic bending hinge is shown in Fig 4.

The post-simplification mechanical model is shown in Fig 5.

### 4. Stagnation point analysis

If both ends of each straight pipeline did not be constricted by the anchor block, the axial elongation induced by thermal expansion can be observed at both ends of the pipeline. Due to the

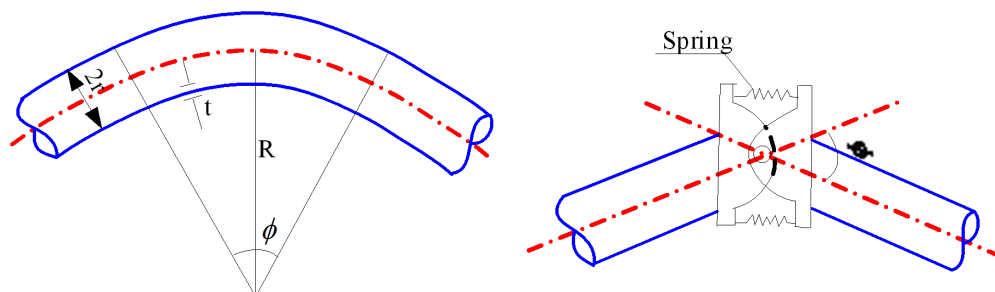


**Fig 4. Simplified model of the elbow.**

doi:10.1371/journal.pone.0150964.g004

different thermal expansion directions between two neighbouring straight pipes near the elbow, bending deformation was generated by push force. Note that, the bending deflection of the straight pipe can disappear rapidly due to the limitation of the anchor block. The deformation mainly occurs near the elbow [10–11].

The derivation of push force of the anchor block follows three assumptions.

1. When thermal expansion occurs, the straight pipe between two elbows elongates to the ends. A point without axial displacement certainly exists along the axial direction of the straight pipeline. The directions of friction force in the two sides between the pipe and the anchor block are opposites. Therefore, a stagnation point must be encountered between the two elbows when thermal expansion occurs.
2. Significant bending deformation can be only observed near the elbow. This deformation decreases rapidly far away from the elbow. The lateral displacement and deflection angle of the section were neglected; this point is equivalent to anchorage points.
3. The deformation in each straight pipeline is related to the nearest two elbows and straight pipelines. This deformation does not almost have the connection with the distant elbows and straight pipes. As a result, few correlations are determined amongst the positions of stationary points.

## 5. Anchor block push force based on an energy method

According to the virtual work principle [12], the deformations at both ends of a bar generated by actual loads are assumed as a virtual displacement. To solve  $\Delta$  (i.e., the displacement of the section along a specified direction as a result of real loads), the unit force can be applied at this

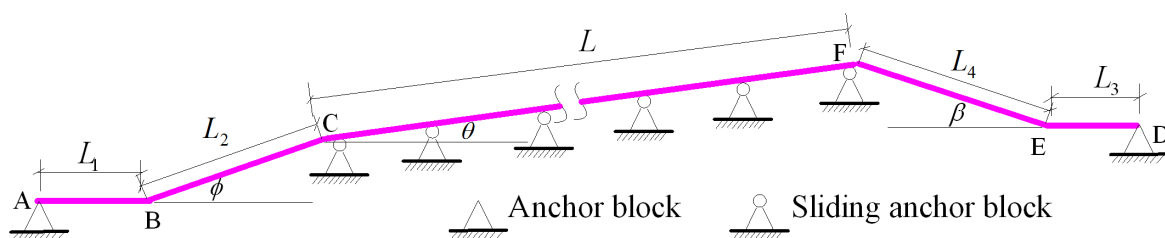


**Fig 5. Mechanical model after simplification.**

doi:10.1371/journal.pone.0150964.g005



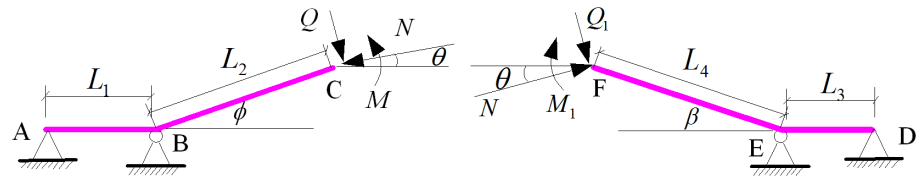


**Fig 6. Internal force of the elbow structure at the entrance and the exit.**

doi:10.1371/journal.pone.0150964.g006

point. The internal forces of the cross-section induced by the unit force are represented by  $\bar{N}$  and  $\bar{M}$ . The virtual work principle of the bar is given by

$$1 \cdot \Delta = \int_l (\bar{N} d\delta + \bar{M} d\theta). \quad (4)$$

Eq (4) is the general expression equation of the displacement of the bar using the unit force method. The displacement generated by a real load is treated as virtual displacement [13–14], and the virtual unit force is taken as the load when the virtual displacement principle is applied. The equation, used to solve the displacement of the linear elastic body based on the unit force method, is given by

$$1 \cdot \Delta = \int_0^l \bar{N} \frac{N dx}{EA} + \int_0^l \bar{M} \frac{M dx}{EI}. \quad (5)$$

### 5.1. Construction of a statically indeterminate model at an elbow

Considering the effect of soil reaction force [15–16] on the sections of AB and DE, the vertical displacements of points B and E are restricted. Therefore, a vertical restraint is certainly set on these points. The internal forces of the elbow in points C and F are shown in Fig 6.

Removing the constraints of point B, a statically indeterminate mechanical model of the elbow at the entrance and the exit is established. This model is presented in Fig 7.

Based on the fact that the deflection values of B and E were equal to 0,  $R_B$  and  $R_E$  in the indeterminate structure are obtained.

$$R_B = -\frac{3[M + NL_2 \sin(\varphi - \theta) - QL_2 \sin(\varphi - \theta)]}{2L_1} + Q. \quad (6)$$

$$R_E = -\frac{3[M_1 + NL_4 \sin(\beta + \theta) - Q_1 L_4 \sin(\beta + \theta)]}{2L_3} + Q_1. \quad (7)$$

### 5.2. Research on the joint displacements of points C and F at an elbow using an energy method

The force analysis generated by applying the unit force in points C and F are displayed in Fig 8.

The displacements of points C and F are defined as  $f_c$  and  $f_F$ , respectively. These variables can be expressed as the following formula based on the unit force method. Additionally, the displacements of points C and F are along the axial direction.

$$f_c = N \left[ \frac{L_1 \cos^2 \theta + L_2 \cos^2(\varphi - \theta)}{EA} + \frac{(4L_2^3 + 3L_1 L_2^2) \sin^2(\varphi - \theta) \sin \theta + 4 \sin^2 \theta L_1^3}{12EI} \right] + \Delta_1 + \Delta_2$$

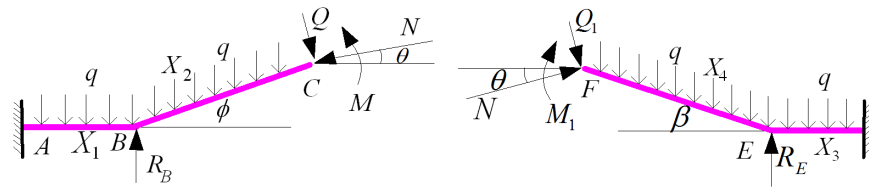


**Fig 7. Statically indeterminate mechanical model of the elbow structure at the entrance and the exit.**

doi:10.1371/journal.pone.0150964.g007

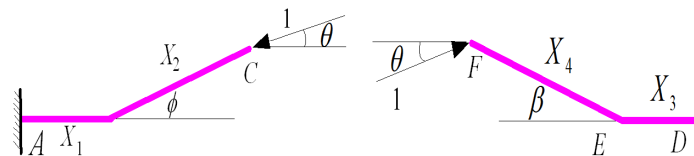


**Fig 8. Elbow structure established by applying unit force to the entrance and the exit.**

doi:10.1371/journal.pone.0150964.g008

$$f_F = N \left[ \frac{L_3 + L_4 \cos^2 \beta}{EA} + \frac{3L_3 L_4^2 \sin^2 \beta + 4L_4^3 \sin^2 \beta}{12EI} \right] + \Delta_3 + \Delta_4,$$

where

$$\Delta_1 = \frac{1}{EA} \left[ QL_2 \sin(\varphi - \theta) \cos(\varphi - \theta) + q \frac{L_2^2}{2} \sin \varphi \cos(\varphi - \theta) \right]$$

$$\Delta_2 = \frac{1}{EI} \left\{ ML_2 \sin(\varphi - \theta) \left( \frac{L_1}{4} + \frac{L_2}{2} \right) - Q \left[ L_2^2 \left( \frac{L_1}{8} + \frac{L_2}{6} \right) \sin(2\varphi - 2\theta) + \frac{L_1^2 L_2}{2} \cos \theta \sin(\varphi - \theta) \right. \right. \\ \left. \left. - \frac{L_1^2 L_2}{2} \sin(\varphi - \theta) - \frac{L_1^3}{6} \sin 2\theta + \frac{L_1^3}{3} \sin \theta \right] - \frac{q L_1^3 L_2}{6} \sin(\varphi - \theta) + \frac{q L_1^4}{8} \sin \theta \right\}$$

$$\Delta_3 = \frac{1}{EA} \left( Q_1 L_4 \sin \beta \cos \beta + q \frac{L_4^2}{2} \sin \beta \cos \beta \right)$$

$$\Delta_4 = \frac{L_4 \sin \beta}{EI} \left[ \left( \frac{L_4}{2} + \frac{L_3}{4} \right) M_1 - \left( \frac{L_4^2 \cos \beta}{3} + \frac{1}{4} L_3 L_4 \cos \beta \right) Q_1 - \frac{q L_3^3}{6} \right]$$

The straight pipeline between two elbows extends to each other, when the pipeline is in expansion case. A point without any axial displacement certainly exists along the axial direction. The direction of support friction on either end of the point is opposite that of soil friction. This point is called the stagnation point. Assuming that the distance between the stagnation point of and point C is  $L_5$ , and the distance between this point and point F is  $L_6$ . Under pressure  $P$  and axial force  $N$ , the displacement of  $\mu_c$  can be determined as follow:

$$u_c = \alpha \Delta t (L_1 \cos \theta + L_2 \cos(\phi - \theta) + L_5) - \frac{N}{EA} (L_1 \cos \theta + L_2 \cos(\phi - \theta) + L_5) \\ + (1 - 2\nu) \frac{\pi r^2 P}{EA} (L_1 \cos \theta + L_2 \cos(\phi - \theta) + L_5).$$

At point C, the displacement also satisfies the deformation compatibility condition, i.e.,  $f_c = \mu_c$ . Thus,

$$N = \frac{\left(\alpha \Delta t + (1 - 2\nu) \frac{\pi r^2 P}{EA}\right) (L_1 \cos \theta + L_2 \cos(\varphi - \theta) + L_5) - \Delta_1 - \Delta_2}{\Delta_5}. \quad (8)$$

Similarly, using the deformation compatibility condition at point F, i.e.,  $f_F = \mu_F$ , the corresponding equation can be expressed as follow:

$$N = \frac{\left(\alpha \Delta t + (1 - 2\nu) \frac{\pi r^2 P}{EA}\right) (L_3 \cos \theta + L_4 \cos(\beta + \theta) + L_6) - \Delta_3 - \Delta_4}{\Delta_6}. \quad (9)$$

Where:

$$\Delta_5 = \frac{L_1 \cos^2 \theta + L_2 \cos^2(\varphi - \theta)}{EA} + \frac{(4L_2^3 + 3L_1 L_2^2) \sin^2(\varphi - \theta) - 6L_1^2 L_2 \sin(\varphi - \theta) \sin \theta + 4 \sin^2 \theta L_1^3}{12EI} + \frac{L_1 \cos \theta + L_2 \cos(\varphi - \theta) + L_5}{EA}$$

$$\Delta_6 = \frac{L_3 \cos^2 \theta + L_4 \cos^2(\beta + \theta)}{EA} + \frac{(4L_4^3 + 3L_3 L_4^2) \sin^2(\beta + \theta) + 6L_3^2 L_4 \sin(\beta + \theta) \sin \theta + 4 \sin^2 \theta L_3^3}{12EI} + \frac{L_3 \cos \theta + L_4 \cos(\beta + \theta) + L_6}{EA}$$

Summarising the two equations above, it can be obtained as follow:

$$\begin{aligned} & \frac{\left(\alpha \Delta t + (1 - 2\nu) \frac{\pi r^2 P}{EA}\right) (L_1 \cos \theta + L_2 \cos(\varphi - \theta) + L_5) - \Delta_1 - \Delta_2}{\Delta_5} \\ &= \frac{\left(\alpha \Delta t + (1 - 2\nu) \frac{\pi r^2 P}{EA}\right) (L_3 \cos \theta + L_4 \cos(\beta + \theta) + L_6) - \Delta_5 - \Delta_6}{\Delta_6}. \end{aligned} \quad (10)$$

When the soil breakout friction in sections  $L_1$  and  $L_3$  are neglected,  $N$  is the thrust of the anchor block.

### 5.3. Approximate solution of moment and shear

Assuming that no elbow exists in the middle of the slope tunnel pipeline, only one stagnation point exists, and

$$L_5 + L_6 = L. \quad (11)$$

Assuming that the friction forces of the sliding anchor block were loaded uniformly at the pipeline, the deflection equation can be solved according to the one of a buried vertical pipe. Then, the deflection equation of  $\omega$  can be expressed as [17]

$$\omega \cong \begin{cases} \left(\alpha \Delta t L - \frac{\nu q L^2}{2EA}\right) \left(1 - \frac{x}{l_b}\right) \left(1 + \frac{5x}{2l_b}\right) & (0 \leq x \leq l_b) \\ 0 & \end{cases}$$

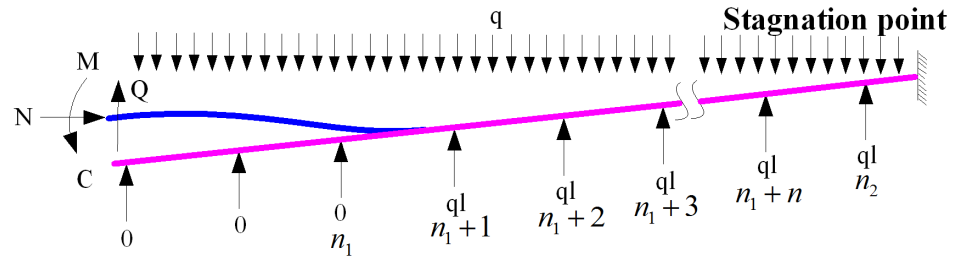


**Fig 9. Calculation of M and Q values after pipeline flexure deformation.**

doi:10.1371/journal.pone.0150964.g009

where  $l_b$  is the approximate location of the first zero point.

$$l_b = \sqrt[4]{\frac{30\sqrt{2}EF\alpha\Delta tLr^2}{\mu q}}.$$

The model, used to solve the values of M and Q, is shown in Fig 9.

$l_a$  is the distance between the deflection point with the values of 0 and the elbow (point C) in the portal and is given by (Zhang et al., 2015)

$$l_a = \sqrt[4]{\frac{30\sqrt{2}EF\alpha\Delta tLr^2}{\mu q}} = \sqrt[4]{\frac{30\sqrt{2}EF\alpha\Delta tL_5r^2}{\mu q}},$$

where  $L_5$  is the distance from the stagnation point to point C.

The following assumption is considered in this analysis. The vertical reaction force in the middle anchor block is calculated with  $F_z = ql$ , and  $l$  is the span between two sliding anchor blocks. Therefore, the shearing force of point C is written as

$$Q = ql_a \cos \theta. \quad (12)$$

Assuming that  $n_1$  is the integer value of  $l_a/l$  and  $n_2$  is the integer value of  $L_5/l$ , the moment of M at the point C can be expressed as

$$M = q \frac{L_5^2 \cos \theta}{2} - ql^2 \frac{(n_2 - n_1)(n_1 + 1 + n_2)}{2} + \frac{ql^2}{12}. \quad (13)$$

$l_b$  is the distance between the deflection point with the values of 0 and elbow (point F) in the opening and is given by

$$l_b = \sqrt[4]{\frac{30\sqrt{2}EF\alpha\Delta tLr^2}{\mu q}} = \sqrt[4]{\frac{30\sqrt{2}EF\alpha\Delta tL_6r^2}{\mu q}},$$

where  $L_6$  is the distance from the stagnation point to point F.

Based on assumption above, the shearing force  $Q_1$  at the point F is written as

$$Q_1 = ql_b \cos \theta. \quad (14)$$

If  $n_3$  is the integer value of  $l_b/l$  and  $n_4$  is the integer value of  $L_6/l$ , then the moment  $M_1$  of point F can be expressed as

$$M_1 = q \frac{L_6^2 \cos \theta}{2} - ql^2 \cos \theta \frac{(n_4 - n_3)(n_3 + 1 + n_4)}{2} + \frac{ql^2}{12}. \quad (15)$$

According to Eqs (10)–(15), six unknown variables ( $M$ ,  $Q$ ,  $M_1$ ,  $Q_1$ ,  $L_5$  and  $L_6$ ) can be solved. The thrust of  $N$  can be solved by substituting the results into Eqs (7) or (8).

#### 5.4. Analytical formula of anchor block push force

In the case of thermal expansion, the straight pipe between two elbows elongates to each other. A point without axial displacement certainly exists along the axial direction. The directions of friction force oppose each other at its two sides. As a result, a stagnation point must be detected between the two elbows when thermal expansion occurs.

The displacement at point C under the effects of temperature difference  $\Delta t$ , pressure  $P$  and axial force  $N$  is indicated by  $u_c$ .

$$u_c = \left[ \alpha \Delta t + (1 - 2\nu) \frac{\pi r^2 P}{EA} \right] [(L_1 \cos \theta + L_2 \cos(\varphi - \theta) + L_5)] - \frac{N}{EA} [(L_1 \cos \theta + L_2 \cos(\varphi - \theta) + L_5)]$$

Considering the friction of the pipe pier, the friction is unrelated to bending moments  $M$  and  $M_1$  when the friction direction passes through points C and F. Eqs (8) and (9) are then written as

$$N = \frac{\left[ \alpha \Delta t + (1 - 2\nu) \frac{\pi r^2 P}{EA} \right] [L_1 \cos \theta + L_2 \cos(\varphi - \theta) + L_5] - \Delta_1 - \Delta_2 - \frac{\mu q L_5^2}{2EA}}{\Delta_5} \quad (16)$$

$$N' = \frac{\left[ \alpha \Delta t + (1 - 2\nu) \frac{\pi r^2 P}{EA} \right] [L_3 \cos \theta + L_4 \cos(\beta + \theta) + L_6] - \Delta_3 - \Delta_4 - \frac{\mu q L_6^2}{2EA}}{\Delta_6} \quad (17)$$

According to the equilibrium equation at the horizontal direction,  $N - \mu q L_5 = N' - \mu q L_6$ , Eqs (16) and (17) can be further expressed as:

$$\begin{aligned} & \frac{\left[ \alpha \Delta t + (1 - 2\nu) \frac{\pi r^2 P}{EA} \right] [L_1 \cos \theta + L_2 \cos(\varphi - \theta) + L_5] - \Delta_1 - \Delta_2 - \frac{\mu q L_5^2}{2EA}}{\Delta_5} - \mu q L_5 \\ &= \frac{\left[ \alpha \Delta t + (1 - 2\nu) \frac{\pi r^2 P}{EA} \right] [L_3 \cos \theta + L_4 \cos(\beta + \theta) + L_6] - \Delta_3 - \Delta_4 - \frac{\mu q L_6^2}{2EA}}{\Delta_6} - \mu q L_6. \end{aligned} \quad (18)$$

Eq (18) can be used to calculate the push force of the anchor block when considering the friction effect of the pipe, instead of Eq (10).

Note that, the stress level is very important to evaluate the safety of the pipeline. Considering the relation of the stress and internal force (i.e., the axial force and bending moment), the axial stress can be solved as follow:

$$\sigma = \frac{N}{A} + \frac{MD}{2I}$$

where  $N$  is the axial force of the pipeline and can be solved based on Eq (17),  $A$  is the area of the cross-section,  $M$  is the bending moment and can be calculated based on Eqs (13) and (15),  $D$  is the external diameter,  $I$  is the moment of inertia.

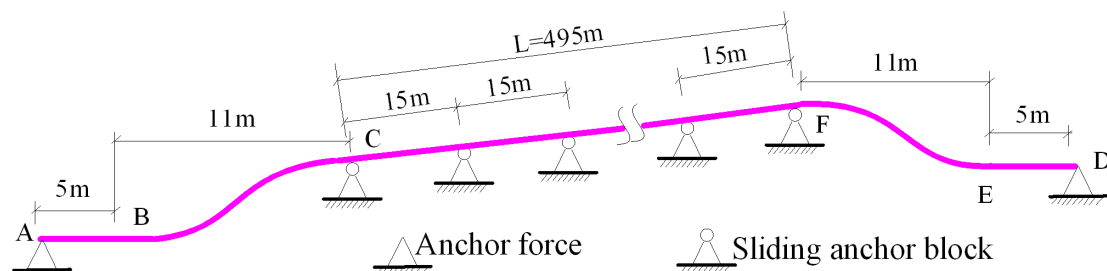


**Fig 10. Integral engineering model of the slope tunnel pipeline.**

doi:10.1371/journal.pone.0150964.g010

## 6. Validation of analytical method

To verify the accuracy of the analytical method, the results of the analytical and the finite element method for the push force of the anchor block of the single-slope tunnel pipeline from the West—East Project are compared. The pipeline is linked to an underground gas storage area containing naturally bedded rock salt. The constructional and integral engineering models of the slope tunnel pipeline are shown in Fig 10. Fig 11 depicts the engineering model in and out of the tunnel opening.

Fig 10 shows the basic parameters of the slope tunnel pipeline. The length of the slope tunnel pipeline is 495 m. Two elbows are inserted into the ground; each end is inserted with an angle of  $30^\circ$ . The anchor block is located at an area where the distance is 5 m from the external elbow. The elbow combination is shown in Fig 11.

The pipeline material is API 5L X80, with the yield and tensile strengths of 485 and 570 MPa, the pipeline diameter of 1219 mm, the wall thicknesses of 18.4, 22 and 26.4 mm, the design pressure of 12 MPa, the temperature difference of  $40^\circ\text{C}$ , the friction factor between the pipeline and the sliding anchor block of 0.6 and the weight per unit length (including the insulation layer, corrosion proofing layer and gas) of 1000 N/m.

Considering the symmetry of the tunnel pipeline structure, the stagnation point is positioned in the middle of the horizontal segment. When the pipeline diameter is equal to 1219 mm, the wall thickness is 18.4 mm. Eqs (12) and (13) indicate that  $Q = 438202.59 \text{ N}$  and  $M = 14687071.875 \text{ N.m}$ . The thrust  $N = 4700801.09 \text{ N}$  is deduced using Eq (16). Tables 1 and 2 list the results of the push force of the anchor block at the entrance and exit under different tunnel gradient varies.

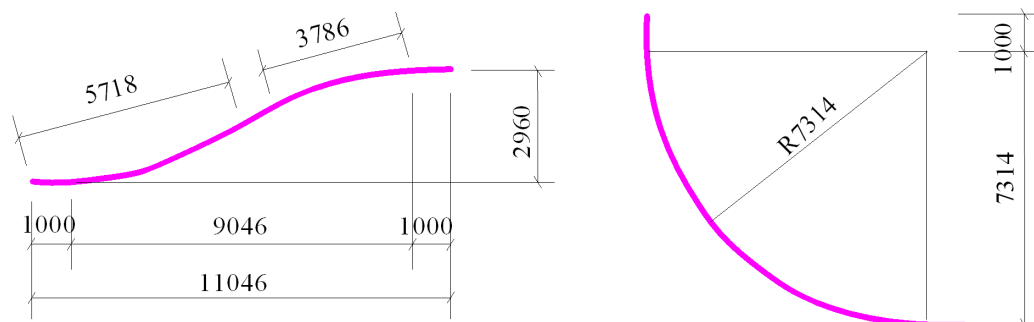


**Fig 11. Local engineering model in and out of the opening.**

doi:10.1371/journal.pone.0150964.g011



**Table 1. Results for push force of anchor block at the tunnel entrance when the tunnel gradient varies.**

Pipeline type	Result for anchor block push force / kN					
	5°	10°	15°	20°	25°	30°
X80, $\phi 1016 \times 14.6$	1701	1558	1409	1202	1013	813
X80, $\phi 1016 \times 17.5$	2189	2018	1842	1618	1381	1144
X80, $\phi 1016 \times 21.0$	2764	2564	2357	2046	1821	1538
X80, $\phi 1016 \times 26.2$	3649	3426	3112	2795	2416	2117

doi:10.1371/journal.pone.0150964.t001

**Table 2. Results for the anchor block push force at the tunnel exit when the tunnel gradient varies.**

Pipeline type	Result for anchor block push force / kN					
	5°	10°	15°	20°	25°	30°
X80, $\phi 1016 \times 14.6$	1762	1634	1512	1356	1231	1112
X80, $\phi 1016 \times 17.5$	2275	2113	1976	1782	1634	1475
X80, $\phi 1016 \times 21.0$	2869	2691	2512	2235	2093	1886
X80, $\phi 1016 \times 26.2$	3765	3574	3297	2998	2703	2496

doi:10.1371/journal.pone.0150964.t002

To verify the accuracy of the analytical method, four finite element software programs (CAESARII, ANSYS, AutoPIPE and ALGOR) were used. According to the engineering model, boundary conditions were concluded as follow: (1) the fixed constraints were used in the locations A and D, respectively. (2) the roller constraints were used in central part of the pipeline. Additionally, the loads were applied based on design parameters, including the inner pressure of 12 MPa and the temperature variation of 40°C.

Tables 3 and 4 depict comparisons of the analytical results with the numerical results calculated with different software programmes.

$\delta$  is the relative error of the analytical and numerical results. The results obtained from AutoPIPE, CAESARII, ALGOR, ANSYS and the analytical formula are equal to  $S_1$ ,  $S_2$ ,  $S_3$ ,  $S_4$

**Table 3. Comparison of anchor block push forces under the operating condition at the tunnel entrance.**

Pipeline type /mm	Result for anchor block push force / kN				Analytical results	Relative error $\delta$
	AutoPIPE	CAESARII	ALGOR	ANSYS		
$\phi 1219 \times 18.4$	2081	1952	1982	2125	2034	3.4%
$\phi 1219 \times 22.0$	2253	2091	2124	2284	2193	3.7%
$\phi 1219 \times 26.4$	2412	2225	2257	2433	2326	4.0%

doi:10.1371/journal.pone.0150964.t003

**Table 4. Comparison of anchor block push force under the operating condition at the tunnel exit.**

Pipeline type	Result for anchor block push force / kN					Relative error $\delta$
	AutoPIPE	CAESARII	ALGOR	ANSYS	Analytical results	
$\phi 1219 \times 18.4$	2371	2221	2253	2413	2314	3.4%
$\phi 1219 \times 22.0$	2543	2392	2431	2581	2491	3.1%
$\phi 1219 \times 26.4$	2742	2534	2572	2782	2662	4.1%

doi:10.1371/journal.pone.0150964.t004

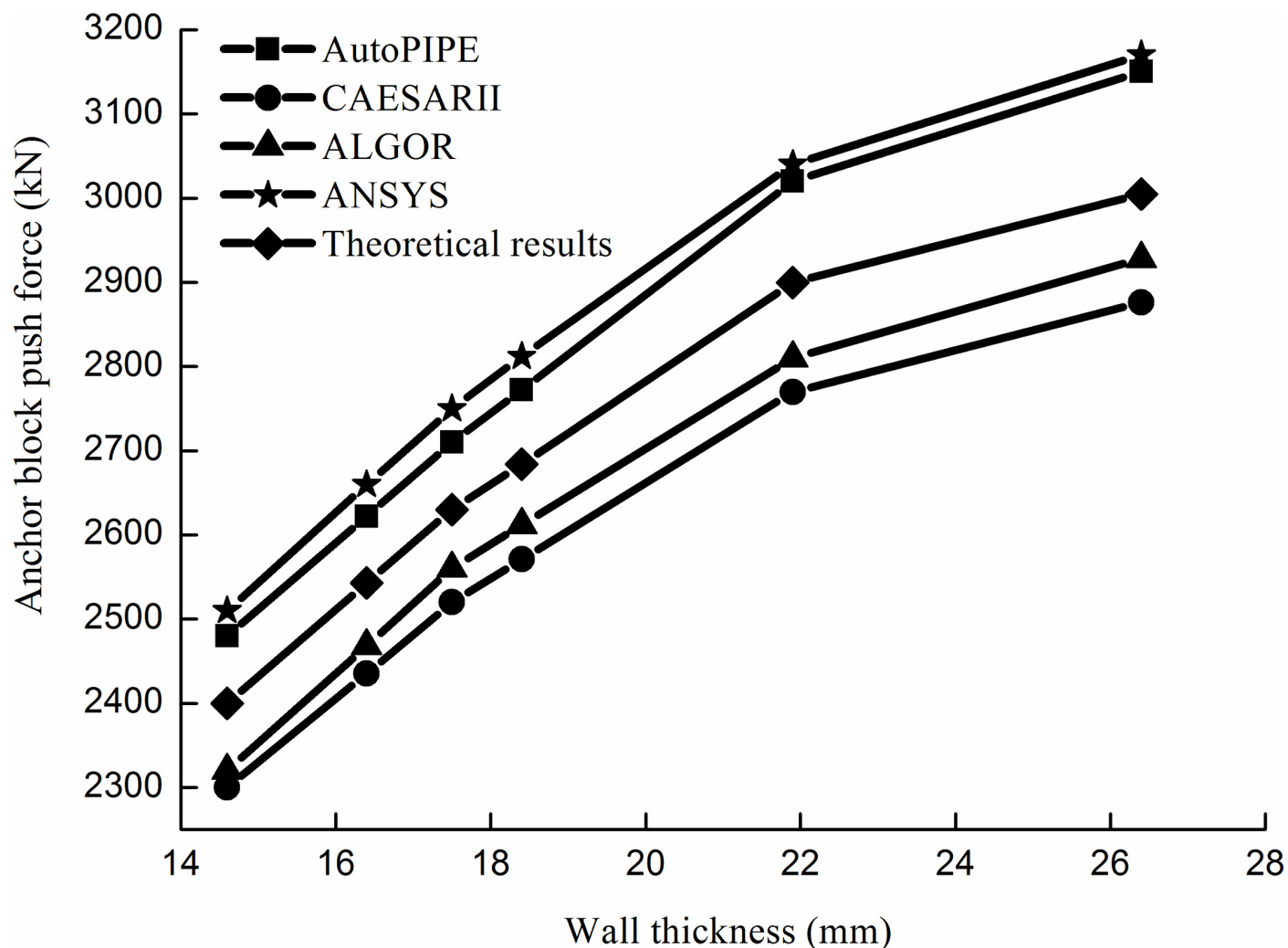


**Fig 12. Block push force results with a pipeline diameter of 1016 mm.**

doi:10.1371/journal.pone.0150964.g012

and  $S$ , respectively. Then, this error can be expressed as:

$$\delta = \sqrt{\frac{(S_1 - S)^2 + (S_2 - S)^2 + (S_3 - S)^2 + (S_4 - S)^2}{4}} / \frac{(S_1 + S_2 + S_3 + S_4)}{4}.$$

The push force of the anchor block increases with an increase of pipe diameter and thickness. The relation between these variables is approximately linear. Considering that the tunnel pipeline is not symmetric in this example, the stagnation point is not located at the middle of the slope tunnel, positioning 220 m from point C. The stagnation point between 220/495 and the angle of two elbows (24/60) is approximately equal.

Figs 12 and 13 shows the comparisons of the results between the analytical method and the numerical method for the push force of the anchor block.

The results show that the analytical and numerical results agree well each other and that the maximum relative error does not exceed 4.1%. Therefore, the results of the analytical method can satisfy engineering requirements.

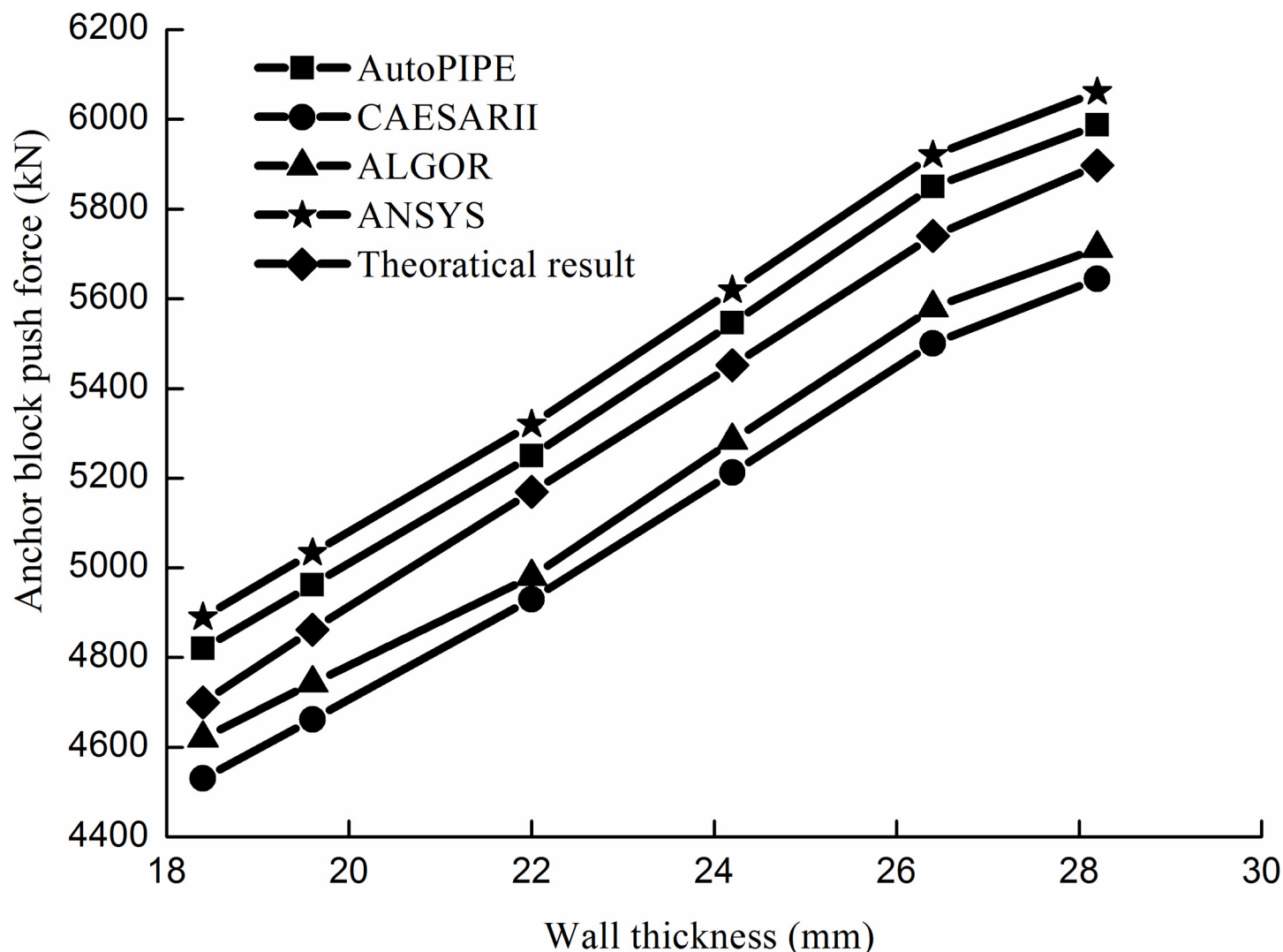


**Fig 13.** Block push force results with a pipeline diameter of 1219 mm.

doi:10.1371/journal.pone.0150964.g013

Additionally, the scene pictures from the West—East Gas Project, China, were shown in Figs 14–21.

## 7. Conclusions

1. According to the actual conditions of pipeline embankment laying at tunnel entrance and exit, the statically indeterminate mechanical modal of bend for tunnel pipeline with anchor blocks subjected to vertical earth pressure and transverse horizontal earth pressure is established. By using unit load method, the axial force of the anchor block for protected pipeline is obtained.
2. The thrust acted on anchor block is calculated by the presented method in this paper for X80 steel tunnel pipeline from West-East Gas Transmission Pipeline Project in China. The





**Fig 14. Anchor blocks at entrances.**

doi:10.1371/journal.pone.0150964.g014



**Fig 15. Anchor blocks at exits.**

doi:10.1371/journal.pone.0150964.g015





**Fig 16. Concrete sliding blocks.**

doi:10.1371/journal.pone.0150964.g016



**Fig 17. Steel sliding blocks.**

doi:10.1371/journal.pone.0150964.g017





**Fig 18. Tunnels.**

doi:10.1371/journal.pone.0150964.g018



**Fig 19. Pipelines.**

doi:10.1371/journal.pone.0150964.g019





**Fig 20. Fixed pipelines.**

doi:10.1371/journal.pone.0150964.g020



**Fig 21. Unfixed pipelines.**

doi:10.1371/journal.pone.0150964.g021

analytical results are compared with finite element results (by CAESAR, AUTOPIPE, PIPE-PAK, ANSYS software), and the maximum relative error is only 4.1%.

3. A code of pipeline design was developed using the method presented. Meanwhile, it has been used in the West—East Gas Project.

## Author Contributions

Analyzed the data: XZY. Contributed reagents/materials/analysis tools: LSZ. Wrote the paper: YFY.

## References

1. Zhang YU, Li HR, Liu DX. Finite element analysis of push force exerted on fixed anchorage near buried piping elbow. *Journal of Dalian University of Technology* 2003; 43(5): 465–466.
2. Palmer AC, Baldry JAS. Lateral Buckling of Axially Constrained Pipelines. *Journal of Petroleum Technology* 2000; 1(6):1283–1284.
3. Wang YJ. Bearing analysis on well fixed pier of heating pipe network buried directly. *Journal of Shenyang Architectural and Civil Engineering Institute* 1998; 14(1):11–12.
4. Al-Gahtani HJ. Optimum design of buried pipeline block anchors. *Practice Periodical on Structural Design and Construction* 2009; 14(4): 190–193.
5. Narasimha RS, Ravi R, Siva PB. Pullout behaviour of suction anchors in soft marine clays. *Marine Georesources and Geotechnology* 1997; 15(2): 95–114.
6. Rao SN, Latha KH, Pallavi B, Surendran S. Studies on pullout capacity of anchors in marine clays for mooring systems. *Applied Ocean Research* 2006; 28(2): 103–111.
7. Irsyam M, Gantina R, Valianti M, Himawan A. Remedial action for the movement of buried gas pipe and anchor block on a very soft soil due to fill embankment. *J. Indonesian Oil Gas Community* 2007; 13–14.
8. Xia ZF. Stress analyzing and approach to designing on upright burying pipeline elbow. *Taiyuan Science and Technology* 2003; 21(6): 36–37.
9. Tong XH, Cui XB, Cai QK. The application of elastic flexure-resisting hinge in the structural analysis of piping systems. *Journal of the University of Petroleum, China* 1989; 13(5): 51–61.
10. Deng DM, Zhang QY, Jin JS. Comparisons of the internal and deflections of aerial crossing pipelines with and without anchor blocks. *J. Oil & Gas Storage and Transportation* 1999; 18(6), 7–20.
11. O'leary PM, Datta SK. Dynamics of buried pipelines. *J. Soil Dynamics and Earthquake Engineering* 1985; 4(3):151–154.
12. An XM. A methods to demonstrate the virtual principles of displacement for variable body. *Journal of China University of Petroleum* 1998; 31(1): 521–524.
13. Dong QL. Virtual work theorem and its application in engineering. *Journal of Henan university* 1997; 27(2):33–34.
14. Luo WD. A generalized virtual work principle of finite elastic body. *Journal of the China University of Petroleum (Edition of Natural Science)* 1999; 23(5): 60–62.
15. Hobbs RE. Pipeline bucking caused by axial loads. *Journal of Constructional Steel Research* 1981; 1(2):4–8.
16. Lee LN, Ariman T, Chen CC. Elastic-plastic bucking of buried pipelines by seismic excitation. *Soil Dynamics and Earthquake Engineering* 1984; 3(4):168–170.
17. Zhang LS, Yan XZ, Yang XJ. Using the unit force method to analyze thrust acting on anchor blocks caused by thermal expansion displacement of X80 tunnel pipelines. *Journal of Pipeline Systems Engineering and Practice* 2015; 7(1): 04015012.